HHS Public Access

Author manuscript

Neurobiol Aging. Author manuscript; available in PMC 2023 September 01.

Published in final edited form as:

Neurobiol Aging. 2022 September ; 117: 189–200. doi:10.1016/j.neurobiolaging.2022.02.015.

CSF Phosphorylated Tau as an Indicator of Subsequent Tau Accumulation

Petrice M. Cogswell[1,*], **Heather J. Wiste**[2], **Michelle M. Mielke**[2,3], **Christopher G. Schwarz**[1], **Stephen D. Weigand**[2], **Val J. Lowe**[1], **Terry M. Therneau**[2], **David S. Knopman**[3], **Jonathan Graff-Radford**[3], **Prashanthi Vemuri**[1], **Matthew L. Senjem**[1,4], **Jeffrey L. Gunter**[1], **Alicia Algeciras-Schimnich**[5], **Ronald C. Petersen**[2,3], **Clifford R. Jack Jr**[1]

[1]Department of Radiology, Mayo Clinic, 200 First St SW, Rochester, MN 55905, USA

[2]Department of Quantitative Health Sciences, Mayo Clinic, 200 First St SW, Rochester, MN 55905, USA

[3]Department of Neurology, Mayo Clinic, 200 First St SW, Rochester, MN 55905, USA

[4]Department of Information Technology, Mayo Clinic, 200 First St SW, Rochester, MN 55905, USA

[5]Department of Laboratory Medicine, Mayo Clinic, 200 First St SW, Rochester, MN 55905, USA

Abstract

We evaluated the relationship between baseline CSF p-tau181 and the rate of tau PET change in the temporal meta-ROI and entorhinal cortex (ERC) and how it varied by amyloid level (CSF Aβ42 or amyloid PET) among 143 individuals from the Mayo Clinic Study of Aging and Mayo Alzheimer Disease Research Center. Higher CSF p-tau181, lower CSF Aβ42, and higher amyloid PET levels were associated with faster rates of tau PET change in both the temporal meta-ROI and ERC. In the temporal meta-ROI, longitudinal tau PET accumulation occurred primarily in participants with abnormal biomarker levels and a diagnosis of dementia, which supports the hypothesis that tau aggregation begins later in the disease process. Compared to the temporal meta-ROI, the ERC showed greater change in tau PET in non-demented participants but less change in later disease stages, supporting ERC as a more sensitive marker of early tau PET changes but with less dynamic range over the disease spectrum. We found both amyloid and

*Corresponding author: 200 First St SW, Rochester, MN 55905, Cogswell.petrice@mayo.edu.

AUTHOR CONTRIBUTIONS

P.M.C. contributed to methodology and writing-original draft. H.J.W. and S.D.W. contributed to methodology, formal analysis designed and writing-review and editing. M.M.M., D.S.K., R.C.P. contributed to conceptualization, resources, and writing-review and editing. C.G.S., M.L.S. and J.L.G. contributed to data curation and writing-review and editing. V.J.L., J.G.R., P.V., and A.A.S. contributed to resources and writing-review and editing. T.M.T. contributed to conceptualization, methodology and writing-review and editing. C.R.J. contributed to conceptualization, methodology, resources, supervision, and writing-review and editing. mmc1.docx

Verification statement: This work was presented in part at the 2021 Alzheimer's Association International Conference. This work has not been previously published, is not under consideration for publication elsewhere, has been approved by all authors, and if accepted with not be published elsewhere in the same form.

CSF p-tau181 were associated with rates of tau PET change but there were some differences in associations by region, amyloid biomarker, and disease stage.

Keywords

Alzheimer Disease; CSF p-tau; amyloid; tau PET

1. INTRODUCTION

The time course over which Alzheimer disease (AD) biomarker levels change, the rate of change, and the associations between biomarkers must be better understood to allow for early diagnosis and treatment. Currently, AD biomarkers of amyloid and tau pathology are most often assessed by CSF or PET but they have different interpretations (Jack et al., 2016, 2018a). CSF measures of amyloid and tau are a result of the of net influx versus efflux of a soluble protein in the CSF compartment, whereas PET standardized uptake values (SUVR) reflect the cumulative burden of aggregated insoluble protein in the brain (Blennow and Hampel, 2003; Gordon et al., 2016).

Relationships between CSF and PET metrics have been studied in various populations for both amyloid and tau. Studies in Alzheimer Disease Research Center (ADRC) and Alzheimer Disease Neuroimaging Initiative (ADNI) participants have shown that CSF amyloid levels decrease as amyloid aggregation in the brain begins (Fagan et al., 2009, 2006; Jagust et al., 2009), and longitudinal decline in CSF amyloid levels may be detected prior to accumulation of amyloid on PET (Palmqvist et al., 2016). Associations between tau pathologic changes on CSF and PET have been recently studied with the more widespread availability of tau PET. Cross-sectional studies have shown modest levels of correlation between CSF phosphorylated tau (p-tau181) and tau PET that are greater in participants with AD than in participants who are cognitively unimpaired (Chhatwal et al., 2016; Gordon et al., 2016; La Joie et al., 2018; Mattsson et al., 2018; Wolters et al., 2020). Based on modeling of cross-sectional data in dominantly inherited and sporadic AD and limited longitudinal data in sporadic AD, changes in CSF p-tau appear to occur prior to detectable tau accumulation on PET (Barthélemy et al., 2020; Mattsson-Carlgren et al., 2020). However, further study of the temporal relationship of CSF p-tau and tau PET in sporadic AD and larger samples of longitudinal data is warranted to better understand disease progression.

Additionally, any modifying effect of amyloid on the relationship of CSF p-tau181 with tau aggregation assessed by PET and the independent value of CSF biomarkers of amyloid and tau must be better understood. Pathologic decreases in CSF Aβ have been shown to occur prior to change in CSF p-tau and accumulation of neocortical tau (Bateman et al., 2012; Donohue et al., 2014; Fagan et al., 2014; Fleisher et al., 2015; Jack et al., 2013, 2010; Pontecorvo et al., 2017) while aggregation of amyloid as measured via PET has been shown to occur more closely in time with rise in CSF p-tau (Bateman et al., 2012). Although changes in amyloid (decrease in CSF Aβ42 and increase in amyloid PET) and increase CSF p-tau have all been shown to be associated with tau aggregation (Barthélemy et al., 2020;

Jack et al., 2020; Mattsson-Carlgren et al., 2020), it is not well understood if CSF p-tau and measures of amyloid provide unique information in predicting rates of tau deposition on PET. Additionally, prior work assessing associations of p-tau with tau PET have been performed using primarily cross-sectional data and, in part, autosomal dominant AD for which specific numeric relationships may not translate directly to longitudinal change in sporadic onset disease. The purpose of this work is to evaluate the relationship between baseline CSF p-tau181 and future tau aggregation measured via longitudinal tau PET and also to assess how that relationship may differ with CSF or PET amyloid level along the continuum of sporadic AD. Given the literature supporting the idea that amyloid biomarkers (CSF and PET) as well as CSF p-tau become abnormal prior to tau PET, the temporality implied in our analyses seems well founded.

2. METHODS

2.1 Participants

This study included participants in the Mayo Clinic Study of Aging (MCSA), a longitudinal cohort study of individuals residing in Olmsted County, Minnesota, or in the Mayo Alzheimer Disease Research Center (ADRC), a longitudinal study of patients enrolled through the clinical practice. To be included in the study, participants were required to have at least two tau PET exams between April 2015 and November 2020, CSF collection at or before the first (baseline) tau PET visit, and a diagnosis of cognitively unimpaired, mild cognitive impairment, or amnestic dementia at the first tau PET visit. Three participants with incomplete or other diagnoses were excluded. CSF was not always collected at the time of the first tau PET scan. Therefore, for 61 (43%) participants we used CSF data collected from up to three years prior to the first tau PET visit. Utilizing the medical history, neurologic examination, and detailed neuropsychological exam, an expert panel determined clinical diagnoses using established criteria (Blacker et al., 1994; Petersen, 2004). Further details of the clinical evaluation have been previously published (Roberts et al., 2008).

2.2 Standard protocol approvals, registrations, and patient consents

The study was approved by the Mayo Clinic and Olmsted Medical Center institutional review boards. Written informed consent was obtained for all participants; consent was obtained from a legally authorized representative for cognitively impaired participants as necessary.

2.3 CSF analysis

CSF was collected via lumbar puncture after overnight fasting and stored in polypropylene tubes at −80°C. CSF hyperphosphorylated tau (p-tau) and β-amyloid 42 (Aβ42) were analyzed using Elecsys p-tau [181P] and Elecsys Aβ [1–42] CSF electrochemiluminescence immunoassays (Roche Diagnostics, Basel, Switzerland). For participants with more than one CSF visit, we used the CSF data collected at or closest to the tau PET visit. Details of CSF collection and storage as well as validation of CSF metrics have previously been described (Van Harten et al., 2020). CSF Aβ42 values were truncated at 1701 pg/mL for 22 participants where the CSF Aβ42 value was greater than the upper technical limit of 1700 pg/mL. Although CSF total-tau (t-tau) was also available in this cohort, our analyses focused

on CSF p-tau181 given the high correlation of these two biomarkers in the cohort (r = 0.98) and the greater specificity of CSF p-tau181 for AD pathologic changes (Blennow, 2017).

2.4 PET imaging and analysis

Tau PET was performed with [18F]flortaucipir (Avid Radiopharmaceuticals) on GE (models Discovery 690XT and Discovery MI) or Siemens scanners (Biograph Vision 600). A longitudinal pipeline with two-compartment partial volume correction (Schwarz et al., 2021), an updated version of the Mayo longitudinal PET pipeline (Schwarz et al., 2019), was used to measure change in tau PET standardized uptake value ratio (SUVR). We studied tau PET in a temporal meta-ROI (amygdala, fusiform, middle/inferior temporal, entorhinal, and parahippocampal regions) which has been shown to best correlate with disease state and separate diagnostic groups (Jack et al., 2017; Lowe et al., 2018). The meta-ROI SUVR was calculated as a voxel number weighted average of the median uptake in each region divided by the median uptake in a composite reference region (eroded supratentorial white matter, pons, and whole cerebellum). A recent thorough evaluation of different longitudinal tau PET methods revealed this to be the optimal method based on effect sizes for separating cognitively unimpaired versus impaired participants and measurement repeatability (Schwarz et al., 2021). We also studied tau PET in the entorhinal cortex region (ERC) as it may be more sensitive to early changes in tau pathology (Braak and Braak, 1991; Kaufman et al., 2018). The baseline tau PET exam was defined as the first available PET and all available subsequent tau PET exams were included in the analysis.

Amyloid PET was performed with Pittsburgh compound B (Klunk et al., 2004) on GE scanners (models Discovery 690XT, Discovery RX, and Discovery MI) and was processed via standard cross-sectional pipelines with SUVR normalized to the cerebellar crus gray matter (Jack et al., 2017). The amyloid PET meta-ROI was composed of the prefrontal, orbitofrontal, parietal, temporal, anterior and posterior cingulate, and precuneus regions. Amyloid PET obtained nearest to the baseline tau PET exam was used. See prior work for further details of the amyloid and tau PET acquisitions (Jack et al., 2017; Schwarz et al., 2021, 2019).

2.5 Cross-sectional statistical analysis

The primary goal of this work was to evaluate associations between CSF p-tau181 and longitudinal changes in tau PET. However, we also performed cross-sectional analyses to confirm that previously demonstrated associations of CSF and PET biomarkers were similarly present in this study population. We used Spearman correlations to assess the strength of associations between baseline CSF p-tau181, CSF Aβ42, and amyloid PET SUVR and tau PET SUVR (computed from the same longitudinal pipeline) for both the temporal meta-ROI and ERC among all participants and within the subset of CU and MCI participants.

2.6 Longitudinal statistical analysis

Before considering both amyloid and PET biomarkers in a single model as predictors of tau aggregation, we used Spearman correlations to assess the strength of associations between each of the predictor variables — CSF p-tau181, CSF Aβ42, and amyloid PET SUVR —

and within-person annual percent change in tau PET in the temporal meta-ROI and ERC. To estimate this within-person annual percent change in tau PET SUVR, we fit a linear regression model for each person using log-transformed SUVR as the outcome and time from baseline scan as the predictor. The use of the log-transformation reduces skewness, stabilizes variability, and allows us to interpret the slope coefficient as annual percent change in tau PET.

For the primary analysis, we fit longitudinal linear mixed effects models to assess the associations between CSF p-tau181 and rate of tau PET accumulation and to evaluate if these associations differed by amyloid level. We fit models with each CSF Aβ42 and amyloid PET as the amyloid measure and with each the temporal metal-ROI and ERC as the tau PET outcome. We also fit models among all participants and within the subset of CU and MCI participants. The models were fit with log-transformed tau PET SUVR as the dependent variable and years from first tau PET scan as the time variable. CSF p-tau181 and amyloid were the primary predictors. Age at the first tau PET scan (i.e., baseline age), sex, and the duration between CSF p-tau181 to tau PET measurement were included to control for potential confounding effects. The model was parameterized to allow for covariate associations with initial tau PET SUVR and change in tau PET (i.e. interactions with time). Our focus was on predictors of change in tau PET with particular interest in the interaction between CSF p-tau181, amyloid, and time which allowed us to assess differences in the association between CSF p-tau181 and annual percent change in tau PET by amyloid level. CSF p-tau181 and amyloid PET were log-transformed to reduce skewness. The model also included participant-specific random intercepts and slopes. With the use of log-transformation of tau PET SUVR, regression coefficients may be interpreted as annual percent change in tau PET.

2.7 Secondary analyses: CSF p-tau181 to Aβ42 ratio

Because the CSF p-tau181 to Aβ42 ratio is used as a diagnostic biomarker in the clinical setting and because the ratio accounts for differences among individuals based on global differences in central nervous system protein production, we repeated the above analysis using the ratio of CSF p-tau181 to CSF Aβ42, in place of CSF p-tau181 alone.

2.8 Data availability

Numeric data underlying these analyses may be made available to investigators upon reasonable request.

3. RESULTS

3.1 Participants

We identified 594 participants with serial tau PET from 2015–2020, and of these, 143 participants had a CSF collection within 3 years of the baseline tau PET scan. The included 143 participants had a median age of 67 (range 32–94); 87 (61%) were male (Table 1). The majority of participants, 109 (76%), were cognitively unimpaired with diagnoses of MCI in 22 (15%) and amnestic dementia in 12 (8%). In 82 (57%) participants' CSF was collected at the same visit as the first (baseline) tau PET exam, with CSF collection occurring up to

2.9 years prior to the baseline tau PET exam in some participants. Nearly all participants (138, 97%) had amyloid PET and baseline tau PET on the same day with a maximum time between PET scans of 23 days. Of the 143 participants, 106 (74%) had two tau PET exams, 33 (23%) had three exams, and 4 (3%) had four exams. The median time from the first to last tau PET scan was 2.6 years (range 0.9 to 5.1 years).

3.2 Cross-sectional associations among CSF and PET biomarkers

CSF p-tau181 (meta-ROI rho = 0.54, p <0.001; ERC rho = 0.56, p <0.001) and amyloid PET (meta-ROI rho = 0.63, p <0.001; ERC rho = 0.53, p <0.001) were positively associated with baseline tau PET for both the temporal meta-ROI and the ERC, while CSF Aβ42 was negatively associated with baseline tau PET (meta-ROI rho = −0.42, p <0.001; ERC rho = −0.27, p = 0.001) (Figure 1). When considering only CU and MCI participants, most associations remained statistically significant though were attenuated to varying degrees: CSF p-tau181 (meta-ROI rho = 0.43, p <0.001; ERC rho = 0.46, p <0.001), CSF Aβ42 (meta-ROI rho = −0.27, p = 0.002) and amyloid PET (meta-ROI rho = 0.53, p <0.001; ERC rho = 0.40, p < 0.001). However, when only considering participants with a diagnosis of CU or MCI, the association of CSF Aβ42 with ERC tau PET was no longer statistically significant (rho = −0.09, p = 0.29).

Participants with a diagnosis of amnestic dementia had higher CSF p-tau181 (median 29 vs 17 and 16 pg/mL, p <0.001), lower CSF Aβ42 (median 524 vs 1097 and 1133 pg/mL, p = 0.002 and p <0.001), higher amyloid PET (median 2.38 vs 1.40 and 1.38 SUVR, p <0.001), and higher baseline temporal meta-ROI tau PET (1.89 vs 1.21 and 1.15 SUVR, p <0.001) and ERC tau PET (1.74 vs. 1.11 and 1.08 SUVR, p <0.001) values than participants with diagnoses of MCI or CU (Table 1).

3.3 Rate of tau PET SUVR change with age

Individual trajectories of tau PET SUVR by age are shown in Figure 2. Most participants showed an increase in tau PET SUVR over time for both the temporal meta-ROI (73% increasing) and ERC (68% increasing). Rates of change in the temporal meta-ROI were greatest for participants with amnestic dementia with little change in the MCI and CU participants (5.4% per year vs 0.6% and 0.4% per year, p < 0.001). For the ERC, rates remained low in CU but rates tended to be a little higher in MCI compared to CU (0.6% vs. 1.3% per year, p = 0.06) and in amnestic dementia compared to MCI (3.3% vs. 1.3% per year, p = 0.09), indicating more of a gradient in rates across diagnosis groups compared to the temporal meta-ROI.

3.4 Association between biomarkers and rate of tau PET change

Higher CSF p-tau181 (meta-ROI rho = 0.19, p = 0.02; ERC rho = 0.39, p <0.001) and higher amyloid PET (meta-ROI rho = 0.27, p = 0.001; ERC rho = 0.39, p <0.001) were associated with faster rates of tau PET change for both the temporal meta-ROI and the ERC while lower CSF Aβ42 was associated with faster rates of tau PET change (meta-ROI rho = −0.23, p = 0.005; ERC rho = −0.24, p = 0.004) (Figure 3). When limiting the analysis to CU and MCI participants, the associations with temporal meta-ROI tau PET rate of change were attenuated and no longer statistically significant. However, the associations with ERC tau

PET rate of change were similar with or without including the participants with amnestic dementia.

3.5 Linear mixed effects models

In longitudinal modeling, the estimated mean increase in tau PET varied considerably with CSF p-tau181 and amyloid levels. More abnormal levels of both CSF p-tau181 ($p < 0.001$) and amyloid ($p < 0.001$) were associated with higher rates of change in temporal meta-ROI tau PET SUVR, and there was a significant interaction ($p < 0.001$ for time × CSF p-tau181 × amyloid PET and $p = 0.01$ for time × CSF p-tau181 × CSF Aβ42) indicating that the association between higher CSF p-tau181 and faster rates of tau PET depended on amyloid levels (Figure 4 A and C, Supplemental Table 1). Table 2 shows the estimated mean annual percent change in tau PET SUVR for combinations of three exemplar values of CSF p-tau181 and either CSF Aβ42 or amyloid PET. Specifically, mean annual percent change in tau PET SUVR was greatest with higher CSF p-tau181 and lower CSF Aβ42 or higher amyloid PET SUVR (lower right quadrant of the tables).

When we excluded participants with amnestic dementia, the associations of CSF p-tau181 and CSF Aβ42 with change in temporal meta-ROI tau PET were attenuated (Figure 4B, Table 2, Supplemental Table 1). The interaction between CSF p-tau181 and Aβ42 was no longer significant ($p = 0.53$), and while rates of temporal meta-ROI tau PET change still appeared to increase some with higher CSF p-tau181 ($p = 0.10$) and CSF Aβ42 ($p = 0.16$), neither were significantly associated with rates of tau PET change in the model. For the model with amyloid PET, the coefficients were not significantly different among the participants without dementia compared to all participants ($p = 0.21$) and a similar pattern was seen such that higher CSF p-tau181 was associated with greater rates of temporal meta-ROI change when amyloid PET was more abnormal (Figure 4D, Table 2, Supplemental Table 1). However, the interaction of CSF p-tau181 and amyloid PET was not significant ($p = 0.12$) and only amyloid PET was significantly associated with rate of temporal meta-ROI tau PET change ($p = 0.02$).

In the ERC, more abnormal levels of both CSF p-tau181 ($p < 0.001$) and CSF Aβ42 ($p = 0.04$) were associated with higher rates of change in tau PET (Figure 4E, Table 2, Supplemental Table 2). When using amyloid PET instead of CSF Aβ42, more abnormal levels of amyloid were associated with higher rates of change in tau PET ($p < 0.001$) but CSF p-tau181 was not ($p = 0.29$) (Figure 4G, Table 2, Supplemental Table 2). There were no significant interactions between CSF p-tau181 and amyloid in either of these ERC models. The associations of CSF p-tau181 and amyloid with rate of change in ERC tau PET were quite similar when excluding the participants with amnestic dementia (Figure 4 F and H, Table 2, Supplemental Table 2).

Age, sex, and duration between CSF and baseline tau PET measurements were not associated with rates of tau PET change for any of the models with one exception. Among participants without dementia, a 10-year difference in age (i.e. 80 vs. 70) was associated with a 0.3% higher rate of change in ERC tau PET.

Note, results were similar when the models were fit among the subset of participants with CSF and tau PET measured at the same visit (data not shown).

3.6 Association between CSF p-tau181 to Aβ42 ratio and tau PET

The associations between the CSF p-tau181/Aβ42 ratio and baseline or rate of change in temporal meta-ROI tau PET SUVR (Figure 5 A and B) were similar to the associations using CSF p-tau181 alone, although the magnitude of the associations were slighter larger with the CSF p-tau181/Aβ42 ratio (rho = 0.63 [p <0.001] and rho = 0.26 [p = 0.002] for CSF p-tau181/Aβ42 vs rho = 0.54 [p <0.001] and rho = 0.19 [p = 0.02] for CSF p-tau181 alone). In the ERC, the correlations between the CSF p-tau181/Aβ42 ratio and baseline or rate of change in tau PET (Figure 5 E and F) were also very similar to the associations when using CSF p-tau181 alone (rho = 0.55 [p <0.001] and rho = 0.41 [p <0.001] for CSF p-tau181/Aβ42 vs rho = 0.56 [p <0.001] and rho = 0.39 [p <0.001] for CSF p-tau181 alone).

In the linear mixed effects model, both amyloid PET (p = 0.03) and the CSF p-tau181/Aβ42 ratio (p = 0.002) were associated with rate of change in temporal meta-ROI tau PET (Figure 5C). While the interaction between CSF p-tau181/Aβ42 and amyloid PET was not statistically significant (p = 0.10 for time × CSF p-tau181/Aβ42 × amyloid PET), the pattern was similar to CSF p-tau181 alone. When including only CU and MCI participants, the effects were attenuated and while rates of tau PET change were still higher at more abnormal amyloid PET levels (p = 0.12), there was no association with the CSF p-tau181/Aβ42 ratio (p = 0.53) (Figure 5D). In the ERC, amyloid PET was the primary predictor of rate of change in tau PET for both the models fit among all (p = 0.004) and among the CU and MCI only (p <0.001) (Figure 5 G and H). The CSF p-tau181/Aβ42 ratio was not significantly associated with rate of change in ERC tau PET (p = 0.97 among all, p = 0.41 among CU and MCI). These results were consistent with the models including amyloid PET and CSF p-tau181 alone.

4. DISCUSSION

As longitudinal tau PET data are becoming more widely available, there is an opportunity to better define the relationship between baseline CSF p-tau181 and future tau aggregation measured via tau PET and how that relationship may differ with amyloid level. Understanding the disease mechanisms as well as how to predict tau aggregation more accurately is important in both clinical and research setting as tau aggregation is closely related to cognitive decline. We found that CSF p-tau181, CSF Aβ42, and amyloid PET SUVR were associated with annual percent change in temporal meta-ROI and ERC tau PET SUVR, however, there were some differences in the associations across the different models we fit.

Though not a primary focus of this work, the cross-sectional analyses showed anticipated relationships of CSF p-tau181, CSF Aβ42, and amyloid PET with tau PET and confirmed that results obtained in larger cohorts were similarly present in this study population. Amyloid may become abnormal without tau accumulation, but higher levels of tau PET only occurred in the setting of abnormal CSF Aβ42 and amyloid PET (Jack et al., 2018b, 2019b). Participants with diagnoses of CU and MCI had amyloid levels that spanned the entire range

seen in the study population, but few CU and MCI participants had temporal meta-ROI or ERC tau PET SUVR > 1.5. By comparison, the participants with amnestic dementia all had temporal meta-ROI and ERC tau PET SUVR > 1.5, which is well into the abnormal range of tau PET SUVR. The separation of diagnostic groups by tau PET but overlap in amyloid levels corresponds with known close associations between tau aggregation and cognitive decline and frequent existence of amyloid without abnormal tau (Brier et al., 2016; Johnson et al., 2016; Ossenkoppele et al., 2016).

Our primary interest was to assess the association of biomarker predictors on within-person change in tau PET. Figure 3 showed that higher CSF p-tau181 as well as more abnormal amyloid (lower CSF Aβ42 and higher amyloid PET SUVR) were associated with greater rates of temporal meta-ROI and ERC tau PET aggregation.

Participants with amnestic dementia had the greatest rates of tau PET change and rates of tau PET were notably higher in the temporal meta-ROI region compared to the ERC. As expected, participants with amnestic dementia also had quite abnormal baseline biomarker levels. CU participants showed little, if any, increase on average for both tau PET regions while MCI participants were moderately increasing only in the ERC. These findings agree with prior work showing that the earliest tau PET change occurs in the ERC (Braak and Braak, 1991; Kaufman et al., 2018) and are consistent with tau aggregation not being detectible by tau PET until later in the disease process, after other biomarkers have become abnormal (Mattsson-Carlgren et al., 2020; Pontecorvo et al., 2017; Reimand et al., 2020; Smith et al., 2020). Temporal meta-ROI tau PET showed little change in early disease stages but rapid increased from already high levels in those with dementia (Brier et al., 2016; Johnson et al., 2016). Our findings also reflect that in general participants with greater baseline tau PET levels (i.e. those with amnestic dementia) also had faster rates of change compared to those with lower baseline tau PET levels as has been observed in prior work (Jack et al., 2020, 2018b; Sanchez et al., 2021).

The linear mixed effects models provide a better understanding of the interrelationships of CSF p-tau181 and amyloid level on change in tau PET. The model summaries shown in Figure 4 and Table 2 demonstrate important variation in tau PET rates by CSF p-tau181 and amyloid, but there are some differences with region, amyloid marker, and disease stage. In the temporal meta-ROI, the association between CSF p-tau181 and rate of tau PET change depended on amyloid level. For example, tau PET increased minimally when amyloid was more normal (e.g. 1400 pg/mL or 1.3 SUVR) and was not found to be sensitive to CSF p-tau181 levels. However, at more abnormal amyloid levels, an increase in CSF p-tau181 was associated with faster tau PET accumulation rates, reaching roughly 2.5% per year at 30 pg/mL. When restricting the sample to participants with CU and MCI, the associations of CSF p-tau181 and amyloid with rate of temporal meta-ROI tau PET change were attenuated. This is not unexpected as CU and MCI participants showed low (<1%) annual change in this region on average, in keeping with a close link between cortical tau aggregation and cognitive performance (Brier et al., 2016; Jack et al., 2019a; Johnson et al., 2016). Omitting the participants with amnestic dementia restricts the dynamic range of tau PET change in the temporal meta-ROI. Therefore, associations of biomarkers with tau PET change in the temporal meta-ROI may be difficult to detect among CU and MCI participants using

currently implemented methods. The use of other tau PET regions, such as the ERC, may provide further insight into biomarker changes in early disease stages.

In the ERC, both higher CSF p-tau181 and lower CSF Aβ42 were associated with greater rates of tau PET change, but the CSF p-tau181 and CSF Aβ42 effects were independent of each other, and these results did not differ when restricting the sample to CU and MCI participants. In contrast, when adjusting for amyloid level via amyloid PET, CSF p-tau181 added little additional predictive information. As ERC tau PET SUVR best reflects change early in the disease stage, these findings may indicate that earlier in the disease stage CSF p-tau181 provide less unique information than later in the disease stage, when tau PET aggregation becomes more widespread. Additionally, the relatively high noise levels in the small ERC region may make associations with CSF p-tau181 more difficult to detect.

Our findings provide further support for a temporal ordering in which CSF p-tau181 changes occur prior to tau PET aggregation, as suggested by prior studies using primarily cross-sectional data (Mattsson-Carlgren et al., 2020; Meyer et al., 2020). However, whereas prior work has shown that amyloid and CSF p-tau181 are correlated and therefore may provide similar, or redundant, information regarding future tau aggregation (Mattsson-Carlgren et al., 2020), we generally found that each of these biomarker levels contribute important information in predicting tau PET rates. The exception was when predicting change in ERC tau PET using amyloid PET, where only amyloid was associated with change. In all models, amyloid, assessed by either CSF or PET, was an important predictor of tau PET change which is consistent with prior work showing amyloid is necessary for tau accumulation in the AD spectrum (Bateman et al., 2012; Fagan et al., 2014; Pontecorvo et al., 2017). Our results suggest that amyloid level provides additional information regarding future tau PET accumulation, beyond that provided by CSF p-tau181. Specifically, amyloid is not only necessary for tau accumulation, but as the amyloid level becomes more abnormal, it appears to continue to affect the disease process.

These differences in our results compared to other studies could be due in part to target brain regions, analysis techniques, study population, and sample size. Specifically, we evaluated the interaction of amyloid and CSF p-tau181 on tau accumulation in a larger cohort of sporadic AD with longitudinal tau PET data and considered amyloid as a continuous variable compared to prior work in a smaller cohort with models fit separately for amyloid positive and negative participants (Mattsson-Carlgren et al., 2020).

Although it has been proposed that tau PET rates may plateau at more advanced disease stages, we did not observe this. Rates of tau PET change in the ERC were indeed lower in those with more advanced disease stages compared to rates in the temporal meta-ROI but nevertheless they still tended to be increasing. Lower rates in this region may be partly due to a ceiling effect of tau PET binding in this region or due to the later stage ghost tangles having lower binding efficiency for the tau PET ligand (Moloney et al., 2021). As in other studies, we may not observe a plateau stage in tau PET change as individuals in that advanced stage of disease are too impaired to participate in research imaging exams.

Normalizing CSF p-tau181 by CSF Aβ42 resulted in only slight changes in the associations between CSF p-tau181 and baseline tau PET SUVR and annual change in tau PET, and the ratio did not provide addition mechanistically interesting information. However, small increases in the magnitude of the associations when using the ratio could be important in the setting of clinical trials. In the linear mixed effect models, the association between the CSF p-tau181/Aβ42 ratio and rate of temporal meta-ROI tau PET change was somewhat less dependent on amyloid level, which may be due to the ratio accounting for the amyloid level as well as variable protein production levels (Wiltfang et al., 2007). Although this ratio may be useful in some applications, by normalizing to amyloid some of the effects of tau could also be removed. Further, the CSF p-tau181/Aβ42 ratio provided little additional information in predicting rates of change in ERC tau PET.

The longitudinal tau PET processing pipeline used in this work improves stability in longitudinal measurements (Schwarz et al., 2021), increasing the likelihood that small changes seen over time were due to true change rather than measurement variability. Despite improved longitudinal measures, there were some participants with small decreases in tau PET SUVR over time presumably due to measurement variability. Similar measurement decreases have also been observed in other cohorts (Harrison et al., 2019; Pontecorvo et al., 2019).

There are limitations to this study. Given the invasive nature of CSF collection, the number of participants with CSF in this longitudinal cohort study was low relative to the larger potential group of participants with imaging. In the future, plasma p-tau measures may allow us to study changes in soluble vs aggregated tau in larger sample sizes as plasma is more easily obtained than CSF. While we analyzed CSF p-tau181 in this study, it is possible that different effect sizes would be seen with CSF p-tau217 or CSF p-tau231 based on the disease process and timing of changes in those CSF markers relative to tau accumulation (Barthélemy et al., 2020, 2017). The CSF assay used could also influence the results along with instrumental variation, pre-analytic handling for CSF, and biologic variation (e.g. protein production for CSF). The ratio of CSF Aβ−42/40 has shown to be a better indicator of disease status than CSF Aβ42 (Wiltfang et al., 2007), but CSF Aβ40 was not available in this study. Tau PET was evaluated using a temporal meta-ROI and ERC. These two ROIs should reflect the most commonly involved regions of tau accumulation in early to mid-stage disease (Jack et al., 2018b). Given the temporal and spatial heterogeneity recognized with tau deposition (Ossenkoppele et al., 2016; Whitwell et al., 2018), it is possible that some participants have tau deposition in regions not captured with this metric. By limiting the dementia group to only those with amnestic dementia, we aimed to reduce the possibility of less typical tau patterns. The age range of participants with amnestic dementia ranges from less than 60 years to approximately 80 years, resulting from the inclusion of early onset dementia cases from the ADRC.

Finally, as with other studies, we capture a short piece of an individual’s disease trajectory within the available data for this study. This limits our ability to directly infer temporal ordering of biomarkers. Further, for some individuals the CSF measures were collected up to 3 years before the first tau PET scan. A prior study of patients with dominantly inherited AD showed that p-tau181 levels begin to decline (i.e. become more “normal”) once tau

aggregation on PET begins (Barthélemy et al., 2020). If similar disease trajectories apply to our population, participants with very high levels of tau PET at baseline may have a lower level of CSF p-tau181 than if measured several years prior, which may decrease estimated effect sizes of baseline CSF p-tau181 with subsequent rate of change in tau PET. Despite this potential limitation, statistically significant associations were detected between baseline CSF p-tau181 and subsequent change in tau PET in this sample and adjusting for the time delay between measurements did not change the results.

In conclusion, higher levels of CSF p-tau181 and more abnormal amyloid are associated with greater temporal meta-ROI and ERC tau aggregation, as detected via rates of change on tau PET. Temporal meta-ROI tau PET accumulation occurred primarily in participants with abnormal CSF p-tau181 and amyloid levels and a diagnosis of amnestic dementia, corresponding to temporal meta-ROI tau aggregation being a later event in disease progression. Compared to the temporal meta-ROI, the ERC showed greater change in tau PET in participants without dementia but less change in later disease stages, supporting ERC to be more sensitive to early tau PET changes but have less dynamic range over the disease spectrum. Both CSF p-tau181 and amyloid are important in predicting tau aggregation and disease progression in AD but the associations vary some with brain region, amyloid biomarker, and disease stage. When focusing on the early disease stages, CSF p-tau181 provides little additional predictive information about the rates of tau PET accumulation after taking into account amyloid PET level.

Supplementary Material

Refer to Web version on PubMed Central for supplementary material.

ACKNOWLEDGEMENTS

We would like to greatly thank AVID Radiopharmaceuticals, Inc., for their support in supplying AV-1451 precursor, chemistry production advice, and FDA regulatory cross-filing permission and documentation needed for this work. This work was supported by the National Institutes of Health [U01 AG006786, P50 AG016574, R37 AG011378, RO1 AG041851, R01 NS097495, R01 AG056366].

REFERENCES

Barthélemy NR, Bateman RJ, Marin P, Becher F, Sato C, Lehmann S, Gabelle A, 2017. Tau hyperphosphorylation on T217 in cerebrospinal fluid is specifically associated to amyloid-β pathology. bioRxiv 226977. 10.1101/226977

Barthélemy NR, Li Y, Joseph-Mathurin N, Gordon BA, Hassenstab J, Benzinger TLS, Buckles V, Fagan AM, Perrin RJ, Goate AM, Morris JC, Karch CM, Xiong C, Allegri R, Mendez PC, Berman SB, Ikeuchi T, Mori H, Shimada H, Shoji M, Suzuki K, Noble J, Farlow M, Chhatwal J, Graff-Radford NR, Salloway S, Schofield PR, Masters CL, Martins RN, O'Connor A, Fox NC, Levin J, Jucker M, Gabelle A, Lehmann S, Sato C, Bateman RJ, McDade E, Dominantly Inherited Alzheimer Network, 2020. A soluble phosphorylated tau signature links tau, amyloid and the evolution of stages of dominantly inherited Alzheimer's disease. Nat. Med 26, 398–407. 10.1038/s41591-020-0781-z [PubMed: 32161412]

Bateman RJ, Xiong C, Benzinger TLS, Fagan AM, Goate A, Fox NC, Marcus DS, Cairns NJ, Xie X, Blazey TM, Holtzman DM, Santacruz A, Buckles V, Oliver A, Moulder K, Aisen PS, Ghetti B, Klunk WE, McDade E, Martins RN, Masters CL, Mayeux R, Ringman JM, Rossor MN, Schofield PR, Sperling RA, Salloway S, Morris JC, Dominantly Inherited Alzheimer Network, 2012. Clinical

and biomarker changes in dominantly inherited Alzheimer's disease. N. Engl. J. Med 367, 795–804. 10.1056/NEJMoa1202753 [PubMed: 22784036]

Blacker D, Albert MS, Bassett SS, Go RC, Harrell LE, Folstein MF, 1994. Reliability and validity of NINCDS-ADRDA criteria for Alzheimer's disease. The National Institute of Mental Health Genetics Initiative. Arch. Neurol 51, 1198–1204. 10.1001/archneur.1994.00540240042014 [PubMed: 7986174]

Blennow K, 2017. A Review of Fluid Biomarkers for Alzheimer's Disease: Moving from CSF to Blood. Neurol. Ther 6, 15–24. 10.1007/s40120-017-0073-9 [PubMed: 28733960]

Blennow K, Hampel H, 2003. CSF markers for incipient Alzheimer's disease. Lancet Neurol. 2, 605–613. 10.1016/s1474-4422(03)00530-1 [PubMed: 14505582]

Braak H, Braak E, 1991. Neuropathological stageing of Alzheimer-related changes. Acta Neuropathol. (Berl.) 82, 239–259. 10.1007/BF00308809 [PubMed: 1759558]

Brier MR, Gordon B, Friedrichsen K, McCarthy J, Stern A, Christensen J, Owen C, Aldea P, Su Y, Hassenstab J, Cairns NJ, Holtzman DM, Fagan AM, Morris JC, Benzinger TLS, Ances BM, 2016. Tau and Aβ imaging, CSF measures, and cognition in Alzheimer's disease. Sci. Transl. Med 8, 338ra66. 10.1126/scitranslmed.aaf2362

Chhatwal JP, Schultz AP, Marshall GA, Boot B, Gomez-Isla T, Dumurgier J, LaPoint M, Scherzer C, Roe AD, Hyman BT, Sperling RA, Johnson KA, 2016. Temporal T807 binding correlates with CSF tau and phospho-tau in normal elderly. Neurology 87, 920–926. 10.1212/WNL.0000000000003050 [PubMed: 27473132]

Donohue MC, Jacqmin-Gadda H, Le Goff M, Thomas RG, Raman R, Gamst AC, Beckett LA, Jack CR, Weiner MW, Dartigues J-F, Aisen PS, Alzheimer's Disease Neuroimaging Initiative, 2014. Estimating long-term multivariate progression from short-term data. Alzheimers Dement. J. Alzheimers Assoc 10, S400–410. 10.1016/j.jalz.2013.10.003

Fagan AM, Mintun MA, Mach RH, Lee S-Y, Dence CS, Shah AR, LaRossa GN, Spinner ML, Klunk WE, Mathis CA, DeKosky ST, Morris JC, Holtzman DM, 2006. Inverse relation between in vivo amyloid imaging load and cerebrospinal fluid Abeta42 in humans. Ann. Neurol 59, 512–519. 10.1002/ana.20730 [PubMed: 16372280]

Fagan AM, Mintun MA, Shah AR, Aldea P, Roe CM, Mach RH, Marcus D, Morris JC, Holtzman DM, 2009. Cerebrospinal fluid tau and ptau(181) increase with cortical amyloid deposition in cognitively normal individuals: implications for future clinical trials of Alzheimer's disease. EMBO Mol. Med 1, 371–380. 10.1002/emmm.200900048 [PubMed: 20049742]

Fagan AM, Xiong C, Jasielec MS, Bateman RJ, Goate AM, Benzinger TLS, Ghetti B, Martins RN, Masters CL, Mayeux R, Ringman JM, Rossor MN, Salloway S, Schofield PR, Sperling RA, Marcus D, Cairns NJ, Buckles VD, Ladenson JH, Morris JC, Holtzman DM, Dominantly Inherited Alzheimer Network, 2014. Longitudinal change in CSF biomarkers in autosomal-dominant Alzheimer's disease. Sci. Transl. Med 6, 226ra30. 10.1126/scitranslmed.3007901

Fleisher AS, Chen K, Quiroz YT, Jakimovich LJ, Gutierrez Gomez M, Langois CM, Langbaum JBS, Roontiva A, Thiyyagura P, Lee W, Ayutyanont N, Lopez L, Moreno S, Muñoz C, Tirado V, Acosta-Baena N, Fagan AM, Giraldo M, Garcia G, Huentelman MJ, Tariot PN, Lopera F, Reiman EM, 2015. Associations between biomarkers and age in the presenilin 1 E280A autosomal dominant Alzheimer disease kindred: a cross-sectional study. JAMA Neurol. 72, 316–324. 10.1001/jamaneurol.2014.3314 [PubMed: 25580592]

Gordon BA, Friedrichsen K, Brier M, Blazey T, Su Y, Christensen J, Aldea P, McConathy J, Holtzman DM, Cairns NJ, Morris JC, Fagan AM, Ances BM, Benzinger TLS, 2016. The relationship between cerebrospinal fluid markers of Alzheimer pathology and positron emission tomography tau imaging. Brain J. Neurol 139, 2249–2260. 10.1093/brain/aww139

Harrison TM, La Joie R, Maass A, Baker SL, Swinnerton K, Fenton L, Mellinger TJ, Edwards L, Pham J, Miller BL, Rabinovici GD, Jagust WJ, 2019. Longitudinal tau accumulation and atrophy in aging and alzheimer disease. Ann. Neurol 85, 229–240. 10.1002/ana.25406 [PubMed: 30597624]

Jack CR, Bennett DA, Blennow K, Carrillo MC, Dunn B, Haeberlein SB, Holtzman DM, Jagust W, Jessen F, Karlawish J, Liu E, Molinuevo JL, Montine T, Phelps C, Rankin KP, Rowe CC, Scheltens P, Siemers E, Snyder HM, Sperling R, Contributors, 2018a. NIA-AA Research Framework:

Toward a biological definition of Alzheimer's disease. Alzheimers Dement. J. Alzheimers Assoc 14, 535–562. 10.1016/j.jalz.2018.02.018

Jack CR, Bennett DA, Blennow K, Carrillo MC, Feldman HH, Frisoni GB, Hampel H, Jagust WJ, Johnson KA, Knopman DS, Petersen RC, Scheltens P, Sperling RA, Dubois B, 2016. A/T/N: An unbiased descriptive classification scheme for Alzheimer disease biomarkers. Neurology 87, 539–547. 10.1212/WNL.0000000000002923 [PubMed: 27371494]

Jack CR, Knopman DS, Jagust WJ, Petersen RC, Weiner MW, Aisen PS, Shaw LM, Vemuri P, Wiste HJ, Weigand SD, Lesnick TG, Pankratz VS, Donohue MC, Trojanowski JQ, 2013. Tracking pathophysiological processes in Alzheimer's disease: an updated hypothetical model of dynamic biomarkers. Lancet Neurol. 12, 207–216. 10.1016/S1474-4422(12)70291-0 [PubMed: 23332364]

Jack CR, Knopman DS, Jagust WJ, Shaw LM, Aisen PS, Weiner MW, Petersen RC, Trojanowski JQ, 2010. Hypothetical model of dynamic biomarkers of the Alzheimer's pathological cascade. Lancet Neurol. 9, 119–128. 10.1016/S1474-4422(09)70299-6 [PubMed: 20083042]

Jack CR, Therneau TM, Weigand SD, Wiste HJ, Knopman DS, Vemuri P, Lowe VJ, Mielke MM, Roberts RO, Machulda MM, Graff-Radford J, Jones DT, Schwarz CG, Gunter JL, Senjem ML, Rocca WA, Petersen RC, 2019a. Prevalence of Biologically vs Clinically Defined Alzheimer Spectrum Entities Using the National Institute on Aging-Alzheimer's Association Research Framework. JAMA Neurol. 10.1001/jamaneurol.2019.1971

Jack CR, Wiste HJ, Botha H, Weigand SD, Therneau TM, Knopman DS, Graff-Radford J, Jones DT, Ferman TJ, Boeve BF, Kantarci K, Lowe VJ, Vemuri P, Mielke MM, Fields JA, Machulda MM, Schwarz CG, Senjem ML, Gunter JL, Petersen RC, 2019b. The bivariate distribution of amyloid-β and tau: relationship with established neurocognitive clinical syndromes. Brain J. Neurol 142, 3230–3242. 10.1093/brain/awz268

Jack CR, Wiste HJ, Schwarz CG, Lowe VJ, Senjem ML, Vemuri P, Weigand SD, Therneau TM, Knopman DS, Gunter JL, Jones DT, Graff-Radford J, Kantarci K, Roberts RO, Mielke MM, Machulda MM, Petersen RC, 2018b. Longitudinal tau PET in ageing and Alzheimer's disease. Brain J. Neurol 141, 1517–1528. 10.1093/brain/awy059

Jack CR, Wiste HJ, Weigand SD, Therneau TM, Lowe VJ, Knopman DS, Botha H, Graff-Radford J, Jones DT, Ferman TJ, Boeve BF, Kantarci K, Vemuri P, Mielke MM, Whitwell J, Josephs K, Schwarz CG, Senjem ML, Gunter JL, Petersen RC, 2020. Predicting future rates of tau accumulation on PET. Brain 143, 3136–3150. 10.1093/brain/awaa248 [PubMed: 33094327]

Jack CR, Wiste HJ, Weigand SD, Therneau TM, Lowe VJ, Knopman DS, Gunter JL, Senjem ML, Jones DT, Kantarci K, Machulda MM, Mielke MM, Roberts RO, Vemuri P, Reyes DA, Petersen RC, 2017. Defining imaging biomarker cut points for brain aging and Alzheimer's disease. Alzheimers Dement. J. Alzheimers Assoc 13, 205–216. 10.1016/j.jalz.2016.08.005

Jagust WJ, Landau SM, Shaw LM, Trojanowski JQ, Koeppe RA, Reiman EM, Foster NL, Petersen RC, Weiner MW, Price JC, Mathis CA, Alzheimer's Disease Neuroimaging Initiative, 2009. Relationships between biomarkers in aging and dementia. Neurology 73, 1193–1199. 10.1212/WNL.0b013e3181bc010c [PubMed: 19822868]

Johnson KA, Schultz A, Betensky RA, Becker JA, Sepulcre J, Rentz D, Mormino E, Chhatwal J, Amariglio R, Papp K, Marshall G, Albers M, Mauro S, Pepin L, Alverio J, Judge K, Philiossaint M, Shoup T, Yokell D, Dickerson B, Gomez-Isla T, Hyman B, Vasdev N, Sperling R, 2016. Tau positron emission tomographic imaging in aging and early Alzheimer disease. Ann. Neurol 79, 110–119. 10.1002/ana.24546 [PubMed: 26505746]

Kaufman SK, Del Tredici K, Thomas TL, Braak H, Diamond MI, 2018. Tau seeding activity begins in the transentorhinal/entorhinal regions and anticipates phospho-tau pathology in Alzheimer's disease and PART. Acta Neuropathol. (Berl.) 136, 57–67. 10.1007/s00401-018-1855-6 [PubMed: 29752551]

Klunk WE, Engler H, Nordberg A, Wang Y, Blomqvist G, Holt DP, Bergström M, Savitcheva I, Huang G, Estrada S, Ausén B, Debnath ML, Barletta J, Price JC, Sandell J, Lopresti BJ, Wall A, Koivisto P, Antoni G, Mathis CA, Långström B, 2004. Imaging brain amyloid in Alzheimer's disease with Pittsburgh Compound-B. Ann. Neurol 55, 306–319. 10.1002/ana.20009 [PubMed: 14991808]

La Joie R, Bejanin A, Fagan AM, Ayakta N, Baker SL, Bourakova V, Boxer AL, Cha J, Karydas A, Jerome G, Maass A, Mensing A, Miller ZA, O'Neil JP, Pham J, Rosen HJ, Tsai R, Visani AV, Miller BL, Jagust WJ, Rabinovici GD, 2018. Associations between [18F]AV1451 tau PET

and CSF measures of tau pathology in a clinical sample. Neurology 90, e282–e290. 10.1212/WNL.0000000000004860 [PubMed: 29282337]

Lowe VJ, Wiste HJ, Senjem ML, Weigand SD, Therneau TM, Boeve BF, Josephs KA, Fang P, Pandey MK, Murray ME, Kantarci K, Jones DT, Vemuri P, Graff-Radford J, Schwarz CG, Machulda MM, Mielke MM, Roberts RO, Knopman DS, Petersen RC, Jack CR, 2018. Widespread brain tau and its association with ageing, Braak stage and Alzheimer's dementia. Brain 141, 271–287. 10.1093/brain/awx320 [PubMed: 29228201]

Mattsson N, Smith R, Strandberg O, Palmqvist S, Schöll M, Insel PS, Hägerström D, Ohlsson T, Zetterberg H, Blennow K, Jögi J, Hansson O, 2018. Comparing 18F-AV-1451 with CSF t-tau and p-tau for diagnosis of Alzheimer disease. Neurology 90, e388–e395. 10.1212/WNL.0000000000004887 [PubMed: 29321235]

Mattsson-Carlgren N, Andersson E, Janelidze S, Ossenkoppele R, Insel P, Strandberg O, Zetterberg H, Rosen HJ, Rabinovici G, Chai X, Blennow K, Dage JL, Stomrud E, Smith R, Palmqvist S, Hansson O, 2020. Aβ deposition is associated with increases in soluble and phosphorylated tau that precede a positive Tau PET in Alzheimer's disease. Sci. Adv 6. 10.1126/sciadv.aaz2387

Meyer P-F, Pichet Binette A, Gonneaud J, Breitner JCS, Villeneuve S, ADNI Investigators, 2020. Characterization of Alzheimer Disease Biomarker Discrepancies Using Cerebrospinal Fluid Phosphorylated Tau and AV1451 Positron Emission Tomography. JAMA Neurol. 77, 508. 10.1001/jamaneurol.2019.4749 [PubMed: 31961372]

Moloney CM, Lowe VJ, Murray ME, 2021. Visualization of neurofibrillary tangle maturity in Alzheimer's disease: A clinicopathologic perspective for biomarker research. Alzheimers Dement. 17, 1554–1574. 10.1002/alz.12321 [PubMed: 33797838]

Ossenkoppele R, Schonhaut DR, Schöll M, Lockhart SN, Ayakta N, Baker SL, O'Neil JP, Janabi M, Lazaris A, Cantwell A, Vogel J, Santos M, Miller ZA, Bettcher BM, Vossel KA, Kramer JH, Gorno-Tempini ML, Miller BL, Jagust WJ, Rabinovici GD, 2016. Tau PET patterns mirror clinical and neuroanatomical variability in Alzheimer's disease. Brain J. Neurol 139, 1551–1567. 10.1093/brain/aww027

Palmqvist S, Mattsson N, Hansson O, Alzheimer's Disease Neuroimaging Initiative, 2016. Cerebrospinal fluid analysis detects cerebral amyloid-β accumulation earlier than positron emission tomography. Brain J. Neurol 139, 1226–1236. 10.1093/brain/aww015

Petersen RC, 2004. Mild cognitive impairment as a diagnostic entity. J. Intern. Med 256, 183–194. 10.1111/j.1365-2796.2004.01388.x [PubMed: 15324362]

Pontecorvo MJ, Devous MD, Kennedy I, Navitsky M, Lu M, Galante N, Salloway S, Doraiswamy PM, Southekal S, Arora AK, McGeehan A, Lim NC, Xiong H, Truocchio SP, Joshi AD, Shcherbinin S, Teske B, Fleisher AS, Mintun MA, 2019. A multicentre longitudinal study of flortaucipir (18F) in normal ageing, mild cognitive impairment and Alzheimer's disease dementia. Brain J. Neurol 142, 1723–1735. 10.1093/brain/awz090

Pontecorvo MJ, Devous MD, Navitsky M, Lu M, Salloway S, Schaerf FW, Jennings D, Arora AK, McGeehan A, Lim NC, Xiong H, Joshi AD, Siderowf A, Mintun MA, 18F-AV-1451-A05 investigators, 2017. Relationships between flortaucipir PET tau binding and amyloid burden, clinical diagnosis, age and cognition. Brain J. Neurol 140, 748–763. 10.1093/brain/aww334

Reimand J, Collij L, Scheltens P, Bouwman F, Ossenkoppele R, Alzheimer's Disease Neuroimaging Initiative, 2020. Association of amyloid-β CSF/PET discordance and tau load 5 years later. Neurology 95, e2648–e2657. 10.1212/WNL.0000000000010739 [PubMed: 32913020]

Roberts RO, Geda YE, Knopman DS, Cha RH, Pankratz VS, Boeve BF, Ivnik RJ, Tangalos EG, Petersen RC, Rocca WA, 2008. The Mayo Clinic Study of Aging: Design and Sampling, Participation, Baseline Measures and Sample Characteristics. Neuroepidemiology 30, 58–69. 10.1159/000115751 [PubMed: 18259084]

Sanchez JS, Hanseeuw BJ, Lopera F, Sperling RA, Baena A, Bocanegra Y, Aguillon D, Guzmán-Vélez E, Pardilla-Delgado E, Ramirez-Gomez L, Vila-Castelar C, Martinez JE, Fox-Fuller JT, Ramos C, Ochoa-Escudero M, Alvarez S, Jacobs HIL, Schultz AP, Gatchel JR, Becker JA, Katz SR, Mayblyum DV, Price JC, Reiman EM, Johnson KA, Quiroz YT, 2021. Longitudinal amyloid and tau accumulation in autosomal dominant Alzheimer's disease: findings from the Colombia-Boston (COLBOS) biomarker study. Alzheimers Res. Ther 13, 27. 10.1186/s13195-020-00765-5 [PubMed: 33451357]

Schwarz CG, Gunter JL, Lowe VJ, Weigand S, Vemuri P, Senjem ML, Petersen RC, Knopman DS, Jack CR, 2019. A Comparison of Partial Volume Correction Techniques for Measuring Change in Serial Amyloid PET SUVR. J. Alzheimers Dis. JAD 67, 181–195. 10.3233/JAD-180749 [PubMed: 30475770]

Schwarz CG, Therneau TM, Weigand SD, Gunter JL, Lowe VJ, Przybelski SA, Senjem ML, Botha H, Vemuri P, Kantarci K, Boeve BF, Whitwell JL, Josephs KA, Petersen RC, Knopman DS, Jack CR, 2021. Selecting software pipelines for change in flortaucipir SUVR: Balancing repeatability and group separation. NeuroImage 238, 118259. 10.1016/j.neuroimage.2021.118259 [PubMed: 34118395]

Smith R, Strandberg O, Mattsson-Carlgren N, Leuzy A, Palmqvist S, Pontecorvo MJ, Devous MD, Sr, Ossenkoppele R, Hansson O, 2020. The accumulation rate of tau aggregates is higher in females and younger amyloid-positive subjects. Brain 143, 3805–3815. 10.1093/brain/awaa327 [PubMed: 33439987]

Van Harten AC, Wiste HJ, Weigand SD, Mielke MM, Kremers WK, Eichenlaub U, Batrla-Utermann R, Dyer RB, Algeciras-Schimnich A, Knopman DS, Jack CR, Petersen RC, 2020. CSF biomarkers in Olmsted County: Evidence of 2 subclasses and associations with demographics. Neurology 95, e256–e267. 10.1212/WNL.0000000000009874 [PubMed: 32591471]

Whitwell JL, Graff-Radford J, Tosakulwong N, Weigand SD, Machulda M, Senjem ML, Schwarz CG, Spychalla AJ, Jones DT, Drubach DA, Knopman DS, Boeve BF, Ertekin-Taner N, Petersen RC, Lowe VJ, Jack CR, Josephs KA, 2018. [18F]AV-1451 clustering of entorhinal and cortical uptake in Alzheimer's disease. Ann. Neurol 83, 248–257. 10.1002/ana.25142 [PubMed: 29323751]

Wiltfang J, Esselmann H, Bibl M, Hüll M, Hampel H, Kessler H, Frölich L, Schröder J, Peters O, Jessen F, Luckhaus C, Perneczky R, Jahn H, Fiszer M, Maler JM, Zimmermann R, Bruckmoser R, Kornhuber J, Lewczuk P, 2007. Amyloid beta peptide ratio 42/40 but not A beta 42 correlates with phospho-Tau in patients with low- and high-CSF A beta 40 load. J. Neurochem 101, 1053–1059. 10.1111/j.1471-4159.2006.04404.x [PubMed: 17254013]

Wolters EE, Ossenkoppele R, Verfaillie SCJ, Coomans EM, Timmers T, Visser D, Tuncel H, Golla SSV, Windhorst AD, Boellaard R, van der Flier WM, Teunissen CE, Scheltens P, van Berckel BNM, 2020. Regional [18F]flortaucipir PET is more closely associated with disease severity than CSF p-tau in Alzheimer's disease. Eur. J. Nucl. Med. Mol. Imaging 47, 2866–2878. 10.1007/s00259-020-04758-2 [PubMed: 32291510]

Highlights

- Tau PET rates increased with more abnormal CSF p-tau181, CSF Aβ42, and amyloid PET
- Temporal meta-ROI and ERC tau PET rates were greatest in participants with dementia
- ERC tau PET showed greater rates of change in MCI compared to CU participants
- Both CSF p-tau181 and amyloid are important in predicting temporal tau aggregation
- At early disease stages, the predictive ability of CSF p-tau181 is limited

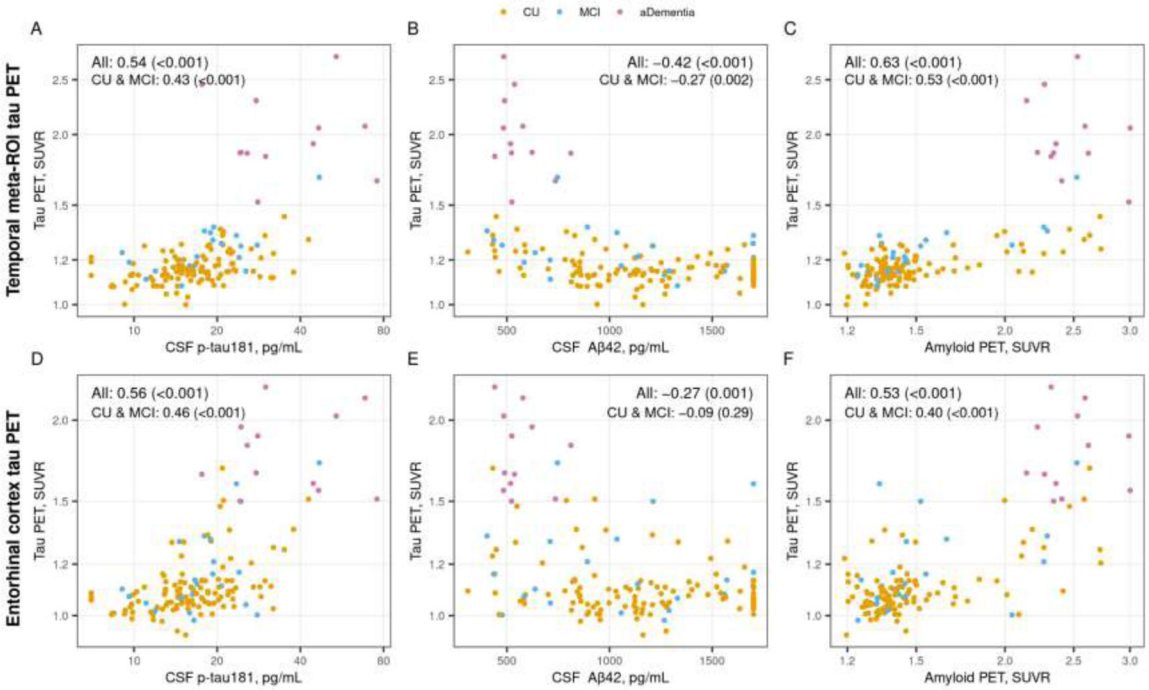

Figure 1 (color figure).

Cross-sectional associations between tau PET and CSF p-tau181, CSF Aβ42, and amyloid PET. Scatter plots of temporal meta-ROI (top row) and entorhinal cortex (ERC, bottom row) tau PET SUVR versus CSF p-tau181 pg/mL (panels A and D), CSF Aβ42 pg/mL (panels B and E), and amyloid PET SUVR (panel C and F) with points colored by clinical diagnosis (orange = cognitively unimpaired [CU], blue = mild cognitive impairment [MCI], and pink = amnestic dementia [aDementia]). Spearman correlations, rho (p value), are shown as a measure of the strength of association among all participants and within the subset of participants who were cognitively unimpaired (CU) or had mild cognitive impairment (MCI).

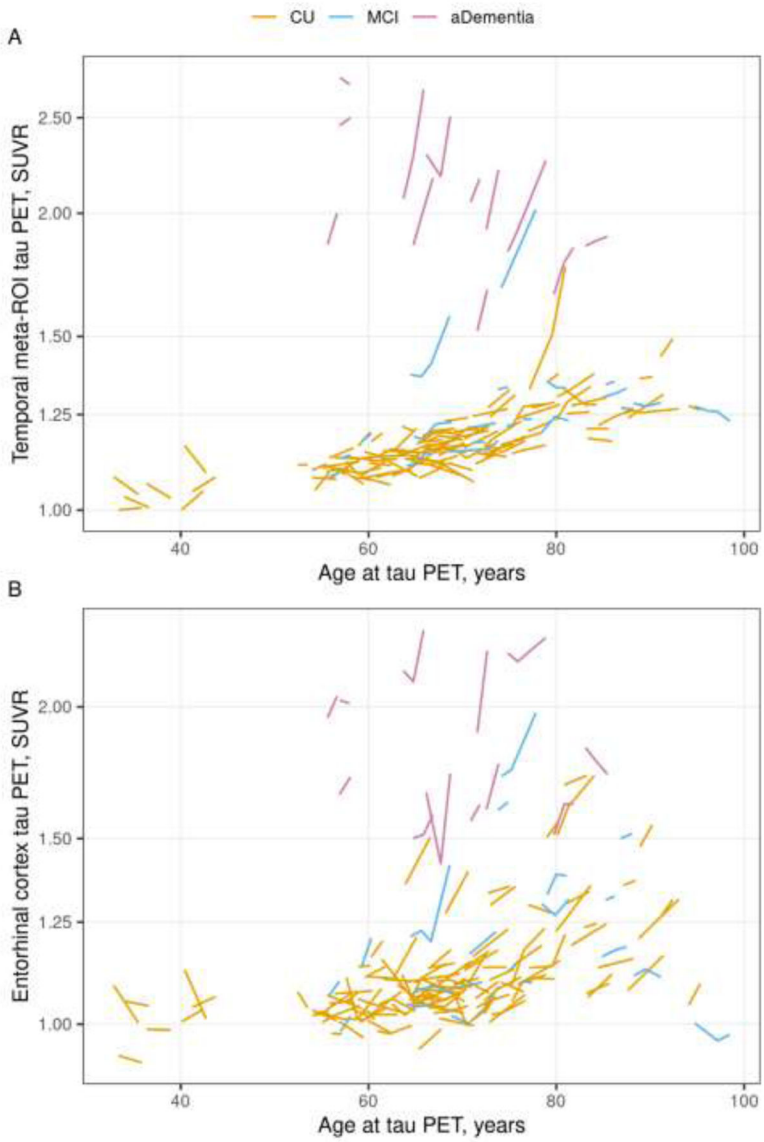

Figure 2 (color figure).

Individual tau PET trajectories by age. Tau PET trajectories within each participant for the temporal meta-ROI (Panel A) and entorhinal cortex (ERC, Panel B) regions by age colored by clinical diagnosis (orange = cognitively unimpaired [CU], blue = mild cognitive impairment [MCI], pink = amnestic dementia [aDementia]). Tau PET is shown on the logarithmic scale.

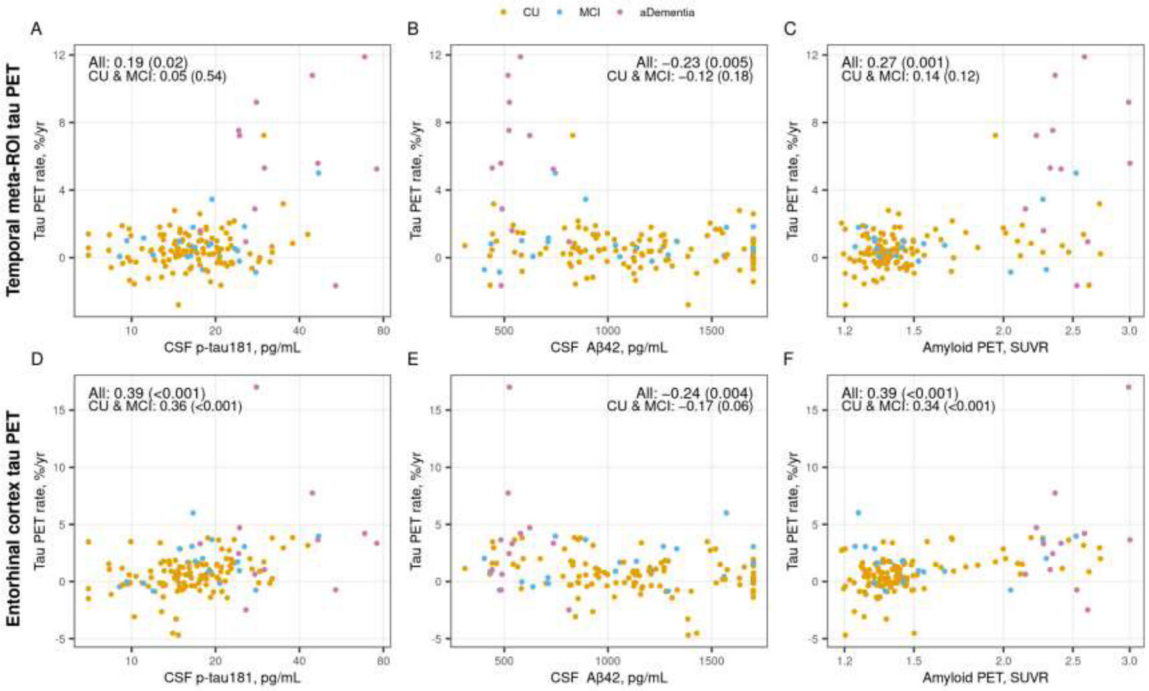

Figure 3 (color figure).

Associations between annual % change in temporal meta-ROI (top row) and entorhinal cortex (ERC, bottom row) tau PET and CSF p-tau181, CSF Aβ42, and amyloid PET. Scatter plots of annual % change in tau PET SUVR versus CSF p-tau181 pg/mL (panels A and D), CSF Aβ42 pg/mL (panels B and E), and amyloid PET SUVR (panels C and F) with points colored by clinical diagnosis (orange = cognitively unimpaired [CU], blue = mild cognitive impairment [MCI], and pink = amnestic dementia [aDementia]). Spearman correlations, rho (p-value), are shown as a measure of the strength of association among all participants and within the subset of participants who were cognitively unimpaired (CU) or had mild cognitive impairment (MCI). The annual % change in tau PET was estimated by fitting a linear regression within each person using all tau PET scans.

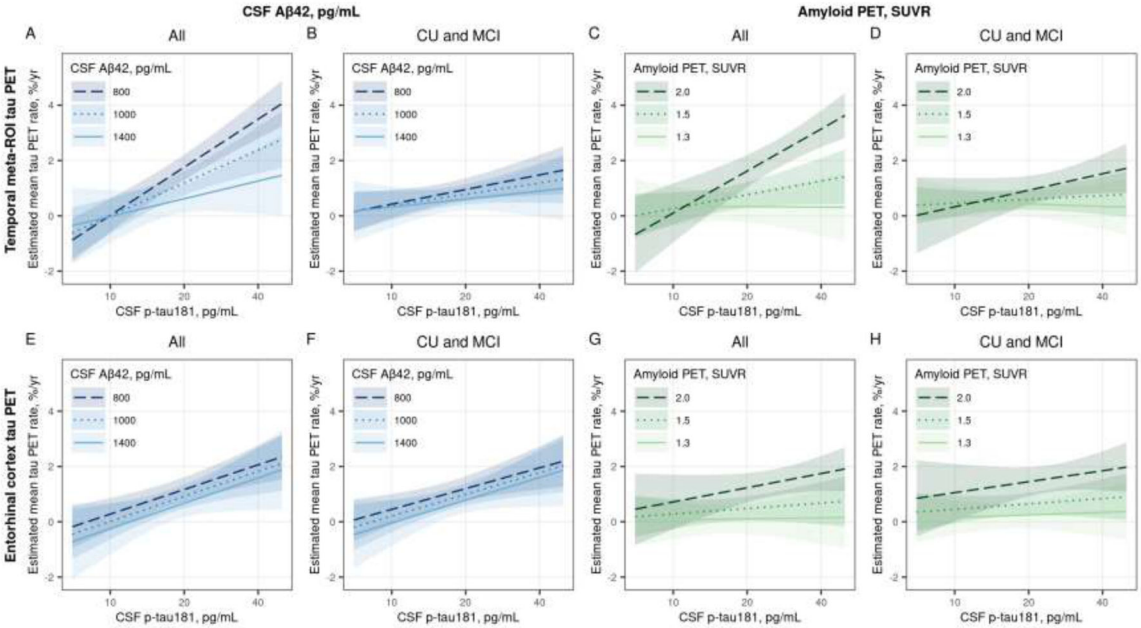

Figure 4 (color figure).

Estimated mean (95% confidence interval) annual % change in temporal meta-ROI (top row) and entorhinal cortex (ERC, bottom row) tau PET by CSF p-tau181 for three exemplar CSF Aβ42 pg/mL (Panels A, B, E, and F) and amyloid PET SUVR (Panels C, D, G, and H) values. Panels A, C, E, and G were estimated among all participants and Panels B, D, F, and H were estimated among participants who were cognitively unimpaired (CU) or had mild cognitive impairment (MCI). Estimates are from linear mixed effects models with log-transformed tau PET SUVR as the outcome and years from first tau PET scan, age, sex, log-transformed CSF p-tau181, and either CSF Aβ42 pg/mL or log-transformed amyloid PET as predictors. The models included years from CSF draw to first tau PET scan to adjust for any delay between the measurements. Subject-specific random intercepts and slopes were also included. The model was parameterized to allow covariate associations with initial tau PET SUVR and change in tau PET (i.e. interactions with time). The model also included an interaction with CSF p-tau181 and amyloid. Estimates are shown for a hypothetical 70-year-old male with no delay between CSF draw and first tau PET scan.

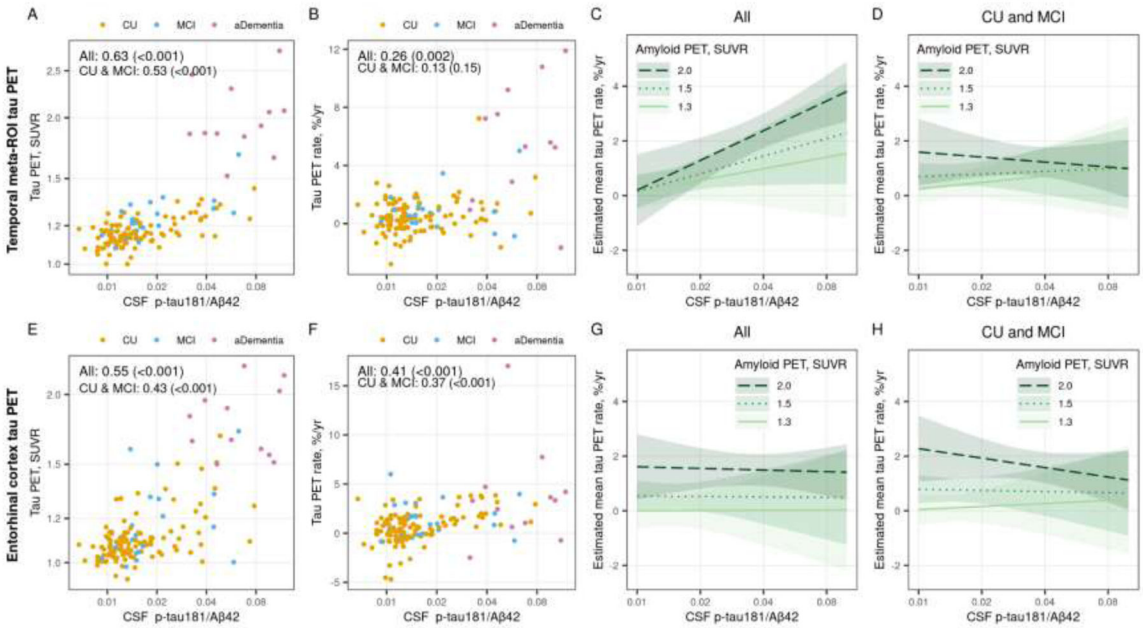

Figure 5 (color figure).

Associations between the CSF p-tau181/Aβ42 ratio and temporal meta-ROI (top row) and entorhinal cortex (ERC, bottom row) tau PET. Scatter plots of CSF p-tau181/Aβ42 versus baseline tau PET SUVR (panel A and E) and annual percent change in tau PET (panel B and F) are shown with points colored by clinical diagnosis (orange = cognitively unimpaired [CU], blue = mild cognitive impairment [MCI], and pink = amnestic dementia [aDementia]). Spearman correlations, rho (p-value), are shown as a measure of the strength of association among all participants and within the subset of participants who were cognitively unimpaired (CU) or had mild cognitive impairment (MCI). Panels C, D, G, and H show the estimated mean (95% confidence interval) annual percent change in temporal meta-ROI and ERC tau PET by CSF p-tau181/Aβ42 for three exemplar amyloid PET SUVR values. Estimates are from a linear mixed effects model fit among all participants (panels C and G) and fit among the subset of CU and MCI participants (panels D and H). The models included log-transformed tau PET SUVR as the outcome and years from first tau PET scan, age, sex, and log-transformed CSF p-tau/Aβ42 as predictors. The model included the duration from CSF draw to first tau PET scan to adjust for any delay between the measurements. The model also included participant-specific random intercepts and slopes. The model was parameterized to allow covariate associations with initial tau PET SUVR and change in tau PET (i.e. interactions with time). The model also included an interaction with CSF p-tau181/Aβ42 and amyloid PET SUVR. Estimates are shown for a hypothetical 70-year-old male with no delay between CSF draw and first tau PET scan.

Table 1.

Table of participant characteristics

Characteristic	Overall (n = 143)	CU (n = 109)	MCI (n = 22)	Amnestic Dementia (n = 12)
Study, n (%)				
MCSA	122 (85%)	109 (100%)	13 (59%)	0 (0%)
ADRC	21 (15%)	0 (0%)	9 (41%)	12 (100%)
Age at tau PET, years				
Median (IQR)	67 (60, 74)	66 (60, 73)	73 (66, 79)	69 (62, 73)
Range	32 to 94	32 to 94	55 to 94	55 to 83
Sex, n (%)				
Female	56 (39%)	51 (47%)	1 (5%)	4 (33%)
Male	87 (61%)	58 (53%)	21 (95%)	8 (67%)
APOE ε4, n (%)				
Non-carrier	96 (68%)	78 (72%)	16 (73%)	2 (17%)
Carrier	46 (32%)	30 (28%)	6 (27%)	10 (83%)
Short Test of Mental Status, median (IQR)	36 (34, 37)	37 (35, 37)	34 (31, 35)	30 (24, 34)
Amyloid PET, SUVR				
Median (IQR)	1.41 (1.33, 1.65)	1.38 (1.32, 1.49)	1.40 (1.33, 1.54)	2.38 (2.31, 2.60)
SUVR ≥1.48	49 (34%)	30 (28%)	7 (32%)	12 (100%)
Tau PET, SUVR *				
Median (IQR)	1.16 (1.13, 1.24)	1.15 (1.12, 1.20)	1.21 (1.15, 1.30)	1.89 (1.85, 2.13)
SUVR ≥1.29	24 (17%)	6 (6%)	6 (27%)	12 (100%)
Entorhinal cortex tau PET, SUVR *				
Median (IQR)	1.09 (1.04, 1.16)	1.08 (1.04, 1.13)	1.11 (1.05, 1.28)	1.74 (1.59, 1.97)
SUVR ≥1.27	29 (20%)	11 (10%)	6 (27%)	12 (100%)
CSF Aβ42, pg/mL **				
Median (IQR)	1100 (801, 1454)	1133 (858, 1519)	1097 (711, 1503)	524 (488, 589)
pg/ml≤1026	65 (45%)	44 (40%)	9 (41%)	12 (100%)
CSF t-tau, pg/mL **				
Median (IQR)	198 (161, 255)	186 (149, 244)	207 (176, 273)	322 (269, 471)
pg/ml≥238	49 (34%)	30 (28%)	9 (41%)	10 (83%)
CSF p-tau, pg/mL **				
Median (IQR)	17 (14, 22)	16 (13, 20)	17 (15, 23)	29 (25, 48)
pg/ml≥22	36 (25%)	19 (17%)	6 (27%)	11 (92%)
Time from CSF to first tau PET scan, years				
Median (IQR)	−0.0 (−0.0, 2.5)	−0.0 (−0.0, 2.5)	−0.0 (−0.0, 1.2)	−0.0 (−0.0, 0.3)
Range	−0.3 to 2.9	−0.3 to 2.9	−0.1 to 2.9	−0.2 to 1.2
Tau PET scans, n (%)				
2	106 (74%)	87 (80%)	13 (59%)	6 (50%)
3	33 (23%)	22 (20%)	5 (23%)	6 (50%)
4	4 (3%)	0 (0%)	4 (18%)	0 (0%)

Characteristic	Overall (n = 143)	CU (n = 109)	MCI (n = 22)	Amnestic Dementia (n = 12)
Time from first to last tau PET scan, years				
Median (IQR)	2.6 (2.1, 3.7)	2.6 (2.4, 3.7)	1.9 (1.1, 2.9)	1.7 (1.0, 2.2)
Range	0.9 to 5.1	1.1 to 5.1	0.9 to 4.2	1.0 to 4.0
Temporal meta-ROI tau PET rate, %/year, median (IQR) *	0.5 (−0.1, 1.4)	0.4 (−0.2, 1.1)	0.6 (0.1, 1.0)	5.4 (2.6, 7.9)
Entorhinal cortex tau PET rate, %/year, median (IQR) *	0.8 (−0.2, 1.7)	0.6 (−0.2, 1.5)	1.3 (0.1, 2.7)	3.3 (0.9, 4.3)

* The tau PET scans were processed with a longitudinal pipeline. SUVR values are summarized for the first tau PET scan.

** The CSF visit is defined as the most recent visit with CSF on or within 3 years prior to the first tau PET visit.

Previously established biomarker cutpoints: CSF t-tau 238 pg/mL, CSF ptau181 22 pg/mL, CSF Aβ42 1026 pg/mL, amyloid PET 1.48 SUVR, temporal meta-ROI tau PET 1.29 SUVR, and entorhinal cortex tau PET 1.27 SUVR.

Table 2 (color table).

Estimated mean annual percent change in tau PET SUVR for combinations of three exemplar values of CSF p-tau181 pg/mL and CSF Aβ42 pg/mL or amyloid PET SUVR. The top rows show estimates for change in the temporal meta-ROI and the bottom rows show estimates for the entorhinal cortex (ERC). The estimates are for the same linear mixed effects model as summarized in Figure 4 and are shown to provide estimates for a variety for exemplar values. Cells with colored backgrounds indicate rates that were significantly increasing with darker colors indicating higher rates. Estimates are shown for a hypothetical 70-year-old male with no delay between the CSF and tau PET measurements and 95% confidence intervals are shown below each estimate. The estimates for females or at other ages would be very similar.

Temporal meta-ROI tau PET

	CSF Aβ42, pg/mL							Amyloid PET, SUVR						
	All			CU and MCI				All			CU and MCI			
	CSF p-tau181, pg/mL			CSF p-tau181, pg/mL				CSF p-tau181, pg/mL			CSF p-tau181, pg/mL			
CSF Aβ42	10	20	30	10	20	30	Amyloid PET	10	20	30	10	20	30	
1400 pg/mL	−0.0 −1.0 to 0.9	0.6 0.1 to 1.1	1.0 0.2 to 1.8	0.3 −0.4 to 1.1	0.6 0.2 to 1.0	0.8 0.1 to 1.4	1.3 SUVR	0.3 −0.4 to 1.1	0.3 −0.2 to 0.9	0.3 −0.5 to 1.1	0.5 −0.1 to 1.1	0.4 −0.0 to 0.9	0.4 −0.3 to 1.0	
1100 pg/mL	−0.0 −0.7 to 0.6	1.2 0.7 to 1.6	1.9 1.2 to 2.5	0.4 −0.1 to 0.9	0.8 0.4 to 1.1	1.0 0.5 to 1.6	1.5 SUVR	0.3 −0.3 to 0.8	0.8 0.3 to 1.2	1.0 0.4 to 1.7	0.5 −0.0 to 0.9	0.6 0.2 to 1.0	0.7 0.1 to 1.2	
800 pg/mL	0.0 −0.6 to 0.6	1.8 1.3 to 2.2	2.8 2.2 to 3.3	0.4 −0.1 to 0.9	1.0 0.5 to 1.4	1.3 0.7 to 1.8	2.0 SUVR	0.1 −1.0 to 1.2	1.6 1.0 to 2.2	2.5 2.0 to 3.0	0.3 −0.7 to 1.4	0.9 0.4 to 1.4	1.3 0.7 to 1.8	

Entorhinal cortex tau PET

	CSF Aβ42, pg/mL							Amyloid PET, SUVR						
	All			CU and MCI				All			CU and MCI			
	CSF p-tau181, pg/mL			CSF p-tau181, pg/mL				CSF p-tau181, pg/mL			CSF p-tau181, pg/mL			
CSF Aβ42	10	20	30	10	20	30	Amyloid PET	10	20	30	10	20	30	
1400 pg/mL	−0.2 −1.2 to 0.7	0.7 0.2 to 1.2	1.2 0.4 to 2.0	−0.0 −0.9 to 0.8	0.8 0.3 to 1.2	1.3 0.5 to 2.0	1.3 SUVR	0.1 −0.6 to 0.8	0.1 −0.4 to 0.7	0.1 −0.6 to 0.9	0.2 −0.5 to 0.8	0.2 −0.2 to 0.7	0.3 −0.4 to 1.0	
1100 pg/mL	0.0 −0.6 to 0.7	0.9 0.5 to 1.4	1.4 0.8 to 2.1	0.2 −0.4 to 0.8	1.0 0.6 to 1.4	1.5 0.9 to 2.0	1.5 SUVR	0.3 −0.3 to 0.8	0.5 0.0 to 0.9	0.6 −0.0 to 1.2	0.5 −0.1 to 1.0	0.6 0.2 to 1.0	0.8 0.2 to 1.3	
800 pg/mL	0.3 −0.3 to 0.9	1.2 0.7 to 1.6	1.7 1.1 to 2.3	0.4 −0.1 to 1.0	1.2 0.8 to 1.6	1.6 1.0 to 2.2	2.0 SUVR	0.7 −0.3 to 1.7	1.2 0.7 to 1.8	1.5 1.0 to 2.0	1.1 0.0 to 2.1	1.4 0.9 to 2.0	1.7 1.1 to 2.2	